EGU2016-6620

Cross comparison of four DPRK events

Dmitry Bobrov, Ivan Kitov, and Mikhail Rozhkov
International Data Centre, CTBTO

CTBTO PREPARATORY COMMISSION | preparatory commission for the comprehensive nuclear-test-ban treaty organization

Introduction. Seismic signals were detected by the IMS seismic network from four announced underground tests conducted by the DPRK in 2006, 2009, 2013, and 2016. These data allow thorough comparison of relative locations, including depth estimates, and magnitudes using several techniques based on waveforms cross correlation. The techniques are still in a development stage and dedicated mostly to the Special Studies and Expert Technical Analysis specified in a Comprehensive Nuclear Test Ban Treaty (CTBT). Seismic signals from these events also provide waveform templates for detection of possible aftershocks with magnitudes by two-to-three units lower than the events themselves. We have processed one month of continuous data after each of four events and detected no aftershocks.

Conclusion. Four DPRK events were conducted within a few kilometers from each other and had sizes within 1 unit of magnitude. Since the ground true information about yields, depths and locations of these events is not available several advanced methods were applied to estimate the observed differences in seismic wave-fields from these events. Waveform cross correlation allows to precisely estimate relative locations and magnitudes of the events close in space. The relative locations of the 2009, 2013 and 2016 DPRK events can be placed within the same mountain. The 2006 event is located at a distance of 2.9 km to east from the 2009 explosion. The depth of burial for the 2016 event is estimated between 650 m and 1100 m by fitting with synthetic seismograms, phase method and cepstral analysis. The depth of 2009 and 2013 are estimated between 400 and 900 m. The 2016 event has also produced an LR-wave with a higher amplitude relative to that measured from the 2013 event likely because of a larger CLVD component. The relative magnitude of four events measured as the logarithm of the RMS-amplitudes in the cross correlation window serves as a reliable measure of the relative size of the DPRK explosions. The relative magnitude estimates are characterized by a lower scattering since the cross correlation coefficient for the signals from four events is higher than 0.8, except a few stations and those for the smallest 2006 event.

Waveform comparison: Similarities and differences

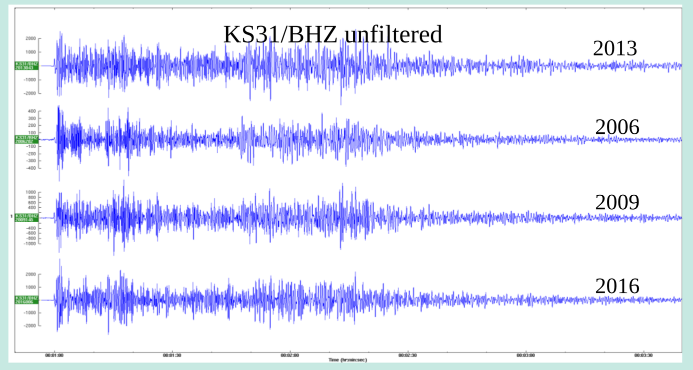

Fig. 1. Unfiltered waveforms recorded at KS31/BHZ from four DPRK events.

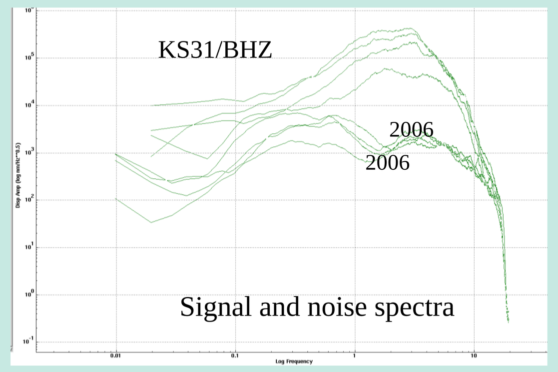

Fig. 2. The spectra of four events (60 s window) and those for the pre-signal noise. For the 2006 DPRK, the noise and signal spectra intersect near 0.5 Hz. For other events, the noise spectra are always below the signal ones.

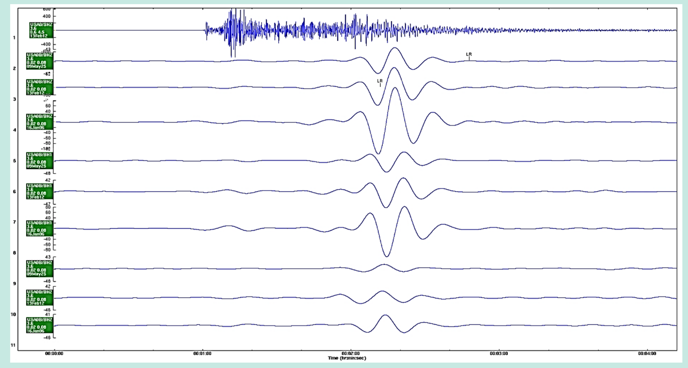

Fig. 5. Station USRK. Comparison of relative amplitudes of the 2009, 2013 and 2016 events. The overall pattern is similar to that observed at KSRS.

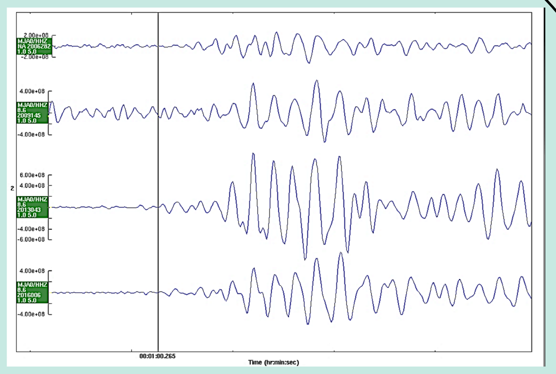

Fig. 6. P-waves from four DPRK events measured at channel MJA0 of IMS array MJAR

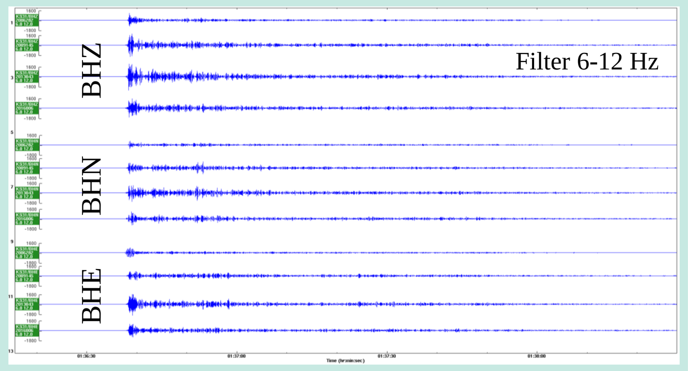

Fig. 3. The 2006 event is relatively richer with higher frequency content at all components. Notice uniform scale for all waveforms. The 2013 DPRK is of higher amplitude than the 2016 one.

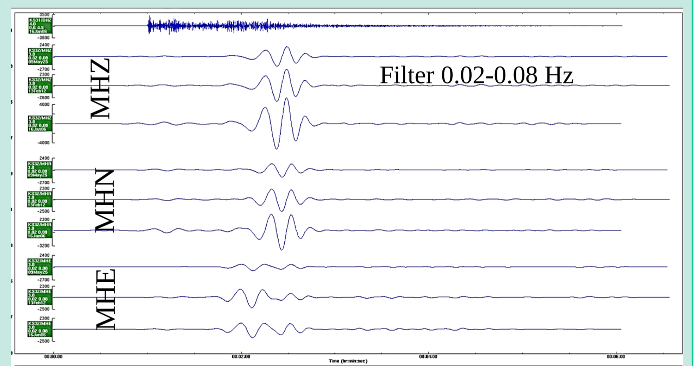

Fig. 4. The relative amplitudes of the 2009 and 2013 events are approximately proportional to their Ms magnitudes. Amplitude of the 2016 event is by a factor of ~1.5 larger than that of the 2013 with the same Ms estimates (see Table 1).

Four DPRK underground explosions conducted in 2006, 2009, 2013, and 2016 were very close in space, and thus, produced similar seismic wave-field at regional and teleseismic distances. This similarity creates a basis for application of advanced methods of data processing like waveform cross correlation for estimation of relative location and magnitude. The depth of burial can also be estimated using cross correlation of the observed and synthetic waveforms as well as cepstral analysis. The depth estimates are also important for interpretation of relative location in the framework of local geology and relief.

The success in application of several techniques proving higher similarities between close sources makes it important to estimate and understand the level of difference between four DPRK tests. First of all, observations at the IMS seismic network demonstrate significant differences in the estimated magnitudes based on body and surface waves as well as local magnitudes, as Table 1 shows. There are several potential sources of these differences: yield, depth of burial, rock type, and local geological structure, which also may affect signal complexity. Since regional seismic wave-field is most sensitive to these parameters it has to be useful for characterization.

Table 1. General information on IDC solutions for four DPRK explosions. NASS – number of associated phases at IMS stations, NDEF – number of defining phases.

JDATE	LAT	LON	DEPTH	NASS	NDEF	MB	MS	ML
2006282	41.312	129.019	0	23	22	4.08	-	3.89
2009145	41.311	129.046	0	89	72	4.51	3.56	4.27
2013043	41.301	129.065	0	151	110	4.92	3.95	4.52
2016006	41.304	129.048	0	165	102	4.82	3.92	4.61

One of the closest regional IMS array station to the DPRK test site is KSRS (4.0 degrees), which detected signals from all four events. IMS station USRK (3.6 degrees) measured only three last events from four. The path to station MJAR at distance (8.6 degrees) has a segment of oceanic crust which makes seismic wave-field quite different from that at the continent.

Figure 1 shows four unfiltered seismograms measured at the broad-band channel KS31/BHZ of IMS array station KSRS. There is general similarity in shape, length and frequency content between these signals. Figure 2 presents eight spectra: four for signals in Figure 1 (60 s window) and four spectra are calculated for the corresponding pre-signal noise also in a 60 s time window.

The corner frequency of signals follow well-known theoretical relationship between yield (magnitude) and source size – the 2006 spectrum has the corner frequency between 5 and 6 Hz and the 2013 spectrum (the highest in amplitude) starts to fall between 2 and 3 Hz. The ratio of 2006/2013 corner frequencies matches the 1 unit of magnitude difference in their body wave magnitudes. All signal and noise spectra intersect near 15 Hz.

Figure 3 illustrates the level of relative difference in high frequency generation. At vertical component, high-frequency content is the highest for the 2013 event, while the 2016 DPRK is approximately at the same level as 2006. At BHN, which is almost orthogonal to the Pn-wave front, the 2006 event has the smallest signal. At BHE, the 2006 is of the same amplitude as the 2009 and 2016 events. Overall, the 2006 Pn-wave is rich with higher frequencies relative to the other DPRK explosions, and thus, it can be best detected using the frequency band between 4 and 8 Hz.

The absolute level of low-frequency noise observed in 2006 is the highest between 4 DPRK events. As a result, the 2006 noise and signal spectra intersect near 0.5 Hz. For other three events, the low-frequency noise spectra are below the signal ones down to 0.01 Hz. This is due to the high-amplitude LR-wave, as illustrated in Figure 4. The absolute amplitudes of LR-wave at three components reveal some differences in the efficiency of surface wave generation. At MHZ and MHN (long period channels with 4 Hz sampling rate), the ratio of LR-wave amplitudes from the 2009 and 2013 is consistent with their Ms estimates. Amplitude of the LR-wave from the 2016 explosion is by a factor of 1.5 larger than that from the 2013 event. Table 1 shows that the 2016 and 2013 Ms magnitudes are almost identical. The higher efficiency of LR generation by the 2016 event is supported by observations at station USRK, which is situated to the north from the DPRK test site. Figure 5 presents corresponding waveforms.

At the E-W broad-band (BH2 for USRK) component, absolute amplitudes of the 2013 and 2016 are almost equal in contrast to Z and N-S components. The difference in generation of vertical, radial and transversal components of surface waves by these three DPRK explosions is likely related to the position of sources within the mountains and type of tectonic stress release. Source mechanisms vary between these three explosions demonstrating different inputs from various components of moment tensor. Based on a recent researches related to the moment tensor estimation of the 2006-2016 DPRK explosions, one may come to the following conclusions. The CLVD component of the moment tensor increased significantly in 2016. For 2013, Whidden&Koper from University of Utah, reported 14% CLVD; Kim, et al. (Korea/Israel/Czech Republic) reported 20% CLVD. For the DPRK 2016, Dreger, et al., reported 36% CLVD and the IDC (EGU, 2016) estimated 43% CLVD. The CLVD is related to tensile failure above the source, which in turn, can be a secondary source of Rg excitation. Therefore, the higher 2016 Rayleigh wave amplitudes are likely connected to the changes in moment tensor.

There is another IMS array MJAR at distance of 8.6 degree from the DPRK test site. Short period sensors of this array do not show low frequency LR-waves. At standard P-wave frequencies between 0.6 Hz and 4.5 Hz, seismic waveforms from four events are very similar.

Depth

Synthetic modeling and cross correlation

We cross compared 3 DPRK events 2009 – 2016 with a method we developed for Special Studies and Expert Technical Analysis (specified in CTBT) based on synthetic modeling with the stationary method approximation (hudson96) [Herrmann and Ammon, 2002] and cross correlating with the observed waveforms. The synthetic waveform with the highest cross correlation corresponds to the appropriate depth of the event. This method allows the use of specific velocity models for the source and receiver as well as the propagation model in between. The source and receiver velocity models are obtained from Crust1.0 and the global reference model ak135 is used for the teleseismic propagation path. To assess the dependency of the amplitude and frequency content of the arrivals, a range of attenuation operators (t*) are chosen and the synthetic waveforms are calculated for a range of source depths from the surface to 4 km, every 100 meters. The synthetic waveforms are then cross correlated with the observed signal.

Figure 11 shows summary of results for several IMS stations indicated at Y axis. Colored diamonds indicate depth corresponding to maximum cross correlation coefficient for search of t* and source depth. Depth histogram shown at bottom of figure. The right-hand column shows examples of the depth determination procedure for selected stations and events. Figure 12 depicts an example of waveform fitting for the indicated station. Observed waveform and best fitting synthetic shown along with optimal depth and t*. Figure 13 shows cross correlation map for range of depths and t*. Warmer colors show higher cross correlation with star indicating highest value. Black contour approximates region of 95% confidence. Cross marginal profiles through depth and t* shown to the side and below. The depth estimates are as follows (columns are median, mean and standard deviation, km, outliers of > 1.6 km are removed, bootstrapping is applied):

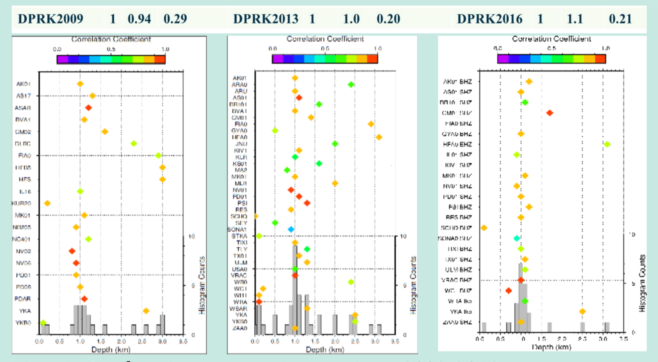

Fig. 11. Depth estimates at various stations: 2009-2016

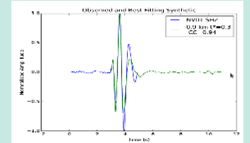

Fig. 12

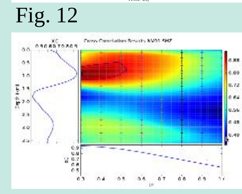

Fig. 13

H (KM)	VP (KM/S)	VS (KM/S)	RHO (GM/CC)	Depth	t*	CC	Rock
1.0	5.38	3.0	2.57	1.0	0.4	0.95	Dolomite or Limestone
1.0	3.17	1.83	2.15	0.6	0.3		Porous and saturated sandstones
1.0	4.17	2.41	2.45	0.7	0.4	0.96	Limestone
1.0	4.573	2.643	2.45	0.7	0.4	0.97	Limestone
1.0	4.573	2.643	2.65	0.8	0.4	0.96	Dolomite or Limestone
1.0	5.0	2.890	2.537	0.9	0.4	0.96	Dolomite or Limestone
1.0	5.1	2.948	2.48	0.9	0.4	0.96	Limestone
1.0	5.17	2.988	2.45	1.0	0.4	0.96	Limestone
1.0	5.18	2.994	2.457, 2.547	1.0	0.4	0.96	Limestone
1.0	5.58	3.225	2.638	1.0	0.4	0.95	Granite
2.0	5.805	3.238	2.66	1.1	0.4	0.95	Granite

Table 2. Coblentz, Pabian, Revised Geologic Site Characterization of the North Korean Test Site at Punggye-ri. Science & Global Security: The Technical Basis for Arms Control, Disarmament, and Nonproliferation Initiatives. Volume 23, Issue 2, 2015.

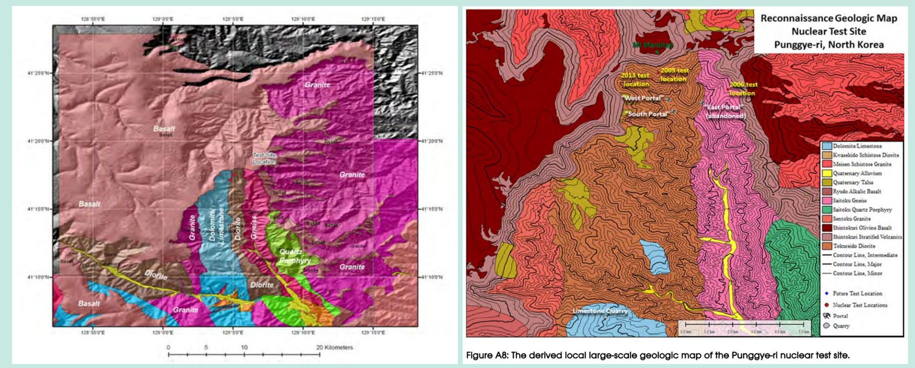

Fig. 14. USGS reconnaissance based geologic interpretation (incorporating ASTER spectral data).

We conducted a study of depth uncertainties based on a an body wave velocity perturbation in upper crustal layer(s). P(S) velocity range was 3.17 (1.83) to 5.805 (3.28). 10 samples for different Vp/Rho/Depth dependencies presented in table below (as in Bourbié, et al., Acoustics of Porous Media, 1987).

Possible rocks constituting upper crustal layer is presented in right column of Table 2. According to (Coblentz, Pabian, 2015) and results of relative location conducted by IDC, NORSAR, KIGAM and some other institutions, this is not quite clear whether or not the DPRK-2016 was conducted in the same geological formation as the DPRK-2009 and 2013. There is a chance that the 2009 and 2013 events were conducted in diorite while 2016 test could be conducted in limestone/dolomite or in stratified volcanic formation. So the depth we produced for the DPRK-2016 could be slightly overestimated when we followed Robert Herrmann's velocity model (upper, green row in a table) and be between 700 and 900 meters. With this if the 2009 and 2013 tests were conducted in a diorite formation then our depth estimate can be underestimate, and real depth of them would be a few hundred meters more than the depth of DPRK-2016.

Phase-only location method

We followed the (Kushnir, et al, 2014) and (Rozhkov, et al, 2016, poster at current EGU session) microseismic event joint hypocenter and focal mechanism determination (so called Phase Method). The method utilizes only phase information of the signal and disregard amplitudes. It was found more robust in noisy environment when mapping hypocenters of sources with signals having SNR << 1 in microseismic hydrofrac monitoring. We used a simplified approach represented by the expression:

$$\Phi=\frac{1}{K}\sum_{k=1}^{K}\left(\frac{1}{\sum_{m=1}^{M}|w_m|}\left\|\sum_{m=1}^{M}\left(e^{i\left(\varphi_{km}+2\pi\tau_m f_k\right)}w_m\right)\right\|\right)$$

where *M* is the number of signals (number of stations plus number of seismic phases recorded at single station), *f* is a frequency, *k* is the number of frequencies, τ is the signal offset, *Wk* is weight corresponding to the theoretical first motion polarity at *Mth* station for certain focal mechanism ([-1,+1]). This method is in a development stage and demonstrates an alternative approach to depth estimation.

Figure 15 compares 2009 – 2016 events depth determination using the Phase Method. Left panel represents special case of the method applied to single stations (IMS network) of the DPRK-2016 event. Mean depth was determined between 1 and 1.1 kilometer with standard deviation of ~ 160 meters. This number is in agreement with the depth determined with the synthetic modeling. Joint depth determination (12 IMS stations at teleseismic distances) gives the depth of 800 meters which is in agreement with estimates produced by other seismic agencies.

Joint processing applied to data of DPRK 2009 and 2013 produce depth with slightly larger depths (1000 and 900 meters) which is in agreement with the results of relative location and position of the day surface projection of these events on a mountain slope. However the resolution of the method depends on the sampling rate of the data, and the modelling error (based on synthetic modeling with ak135 global model) at depths with low P-pP time separation reaches 200 meters at low (20Hz) sampling rates.

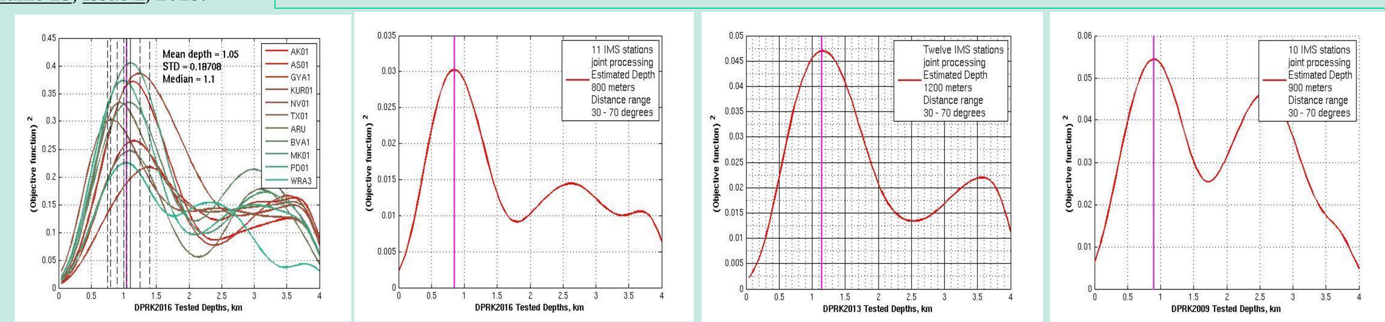

Fig. 15.

Relative location

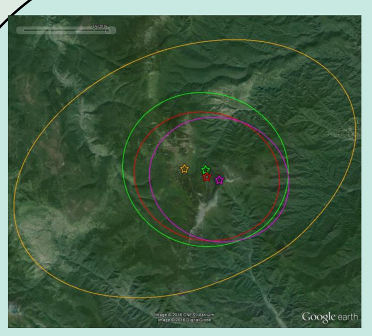

Fig. 7. REB event locations for: 2006 yellow, 2009 green, 2013 magenta, and 2016 red.

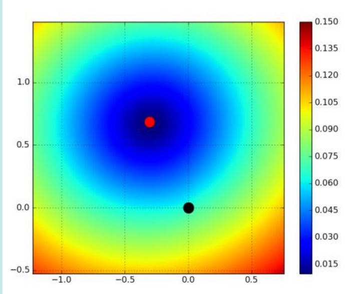

Fig. 8. An example of relative location: the position of the 2016 DPRK event (red dot) relative to that of the 2013 event (black). Distribution of the RMS travel time residuals is shown by colour, scale in seconds.

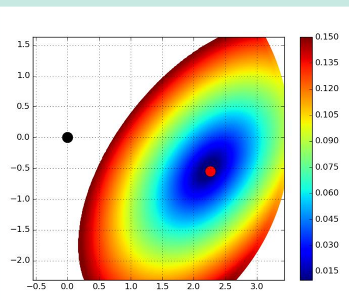

Fig. 9. Relative location: the position of the 2006 DPRK event (red dot) relative to the 2009 event (black). Three regional stations are used.

The IDC has estimated epicentres of four DPRK events using P-wave detections at primary and, when available, auxiliary IMS stations. Table 1 lists four locations from the Reviewed Event Bulletin (REB) and the numbers of associated and defining phases. Figure 7 depicts absolute positions of four epicentres and corresponding confidence ellipses – the biggest is for the 2006 DPRK. It is worth noting that the epicentres are obtained independently and the confidence ellipses represent the areas where actual epicentres reside with 90% probability.

The IMS seismic data from the DPRK 2006, 2009, 2013, and 2016 allow accurate relative location using waveform cross correlation. This procedure uses cross correlation detections and differential travel time residuals. For relative location, the master event is fixed and the travel time residuals at several stations are calculated using their respective theoretical travel times to the master event. The relative location of a slave event is the point on the surface where the RMS travel time residual reaches its minimum.

We use grid search algorithm and calculate travel time residuals for all stations in each node of a grid with 10 m spacing. Figure 8 presents the distribution of the RMS travel time residuals over the grid as obtained using four regional array stations USRK, KSRS, MJAR, and SONM for the DPRK 2013 as a master and the 2016 DPRK as a slave. These stations are characterized by different sampling rates 20 Hz at KSRS, 40 Hz USRK, 50 Hz at SONM, and 80 Hz at MJAR. In order to make the sampling rate, and thus the distance uncertainty associated with discrete timing, uniform over stations and to improve the accuracy of onset time estimation with cross correlation we resample all waveforms to 200 Hz. This rate provides the onset time uncertainty of 0.0025 s, which is equivalent to the source-station distance uncertainty of 20 m for Pn-wave with 8 km/s velocity. Having 4 stations, one can determine the relative location with 10 to 20 m uncertainty. For poor slave signals, however, the uncertainty increases since the onset time can be biased by the ambient noise. In order to retain high quality of signals and to improve SNR we use only IMS arrays in the relative location of four DPRK events.

Figure 8 shows that the 2016 DPRK test was conducted **750** m to north-north-west from the 2013 event. For the original sampling rates at the same stations the estimated distance was **650** with 100 m accuracy. Figure 9 presents the location of the 2006 event relative to the DPRK 2009. The distance is **2.32** km with local coordinates dx=2.26 km and dy=-0.55 km. Hence, the relative location is effective even at ranges of a few km since the level of cross correlation allows precise onset time estimates. The level of cross correlation is discussed later on.

Resampling to 200 Hz also helps to improve the relative location when teleseismic phases are included. The distance uncertainty associated with teleseismic phases is higher because of lower slowness, e.g. the 0.025 s (40 Hz) uncertainty in onset time is equivalent to 375 m uncertainty in epicentral distance for 15 km/s P-wave velocity.

Figures 10a-c depict a series of relative locations based on three (2009-2013-2016) DPRK events separately and the joint relative location using all events as masters and slaves for a given set of stations and sampling rates. Figure 10a presents results for 4 regional stations with their actual sampling rates. Figure 10b displays the same station configuration but for sampling rate 200 Hz, and Figure 10c shows the result of relative location when all stations with detections from 4 DPRK events are used and their waveforms are resampled to 200 Hz. The latter case provides the most reliable and stable relative locations for the latter three events, but is poor for the 6 when teleseismic signals are weak. For smaller events in the same area, e.g. aftershocks or explosions in large underground cavities (cavity decoupled explosions), it is most likely that signals at only closest regional stations will be available. Therefore, the case 10b is the most important for the comprehensive monitoring of underground nuclear tests as providing the highest resolution and reliability.

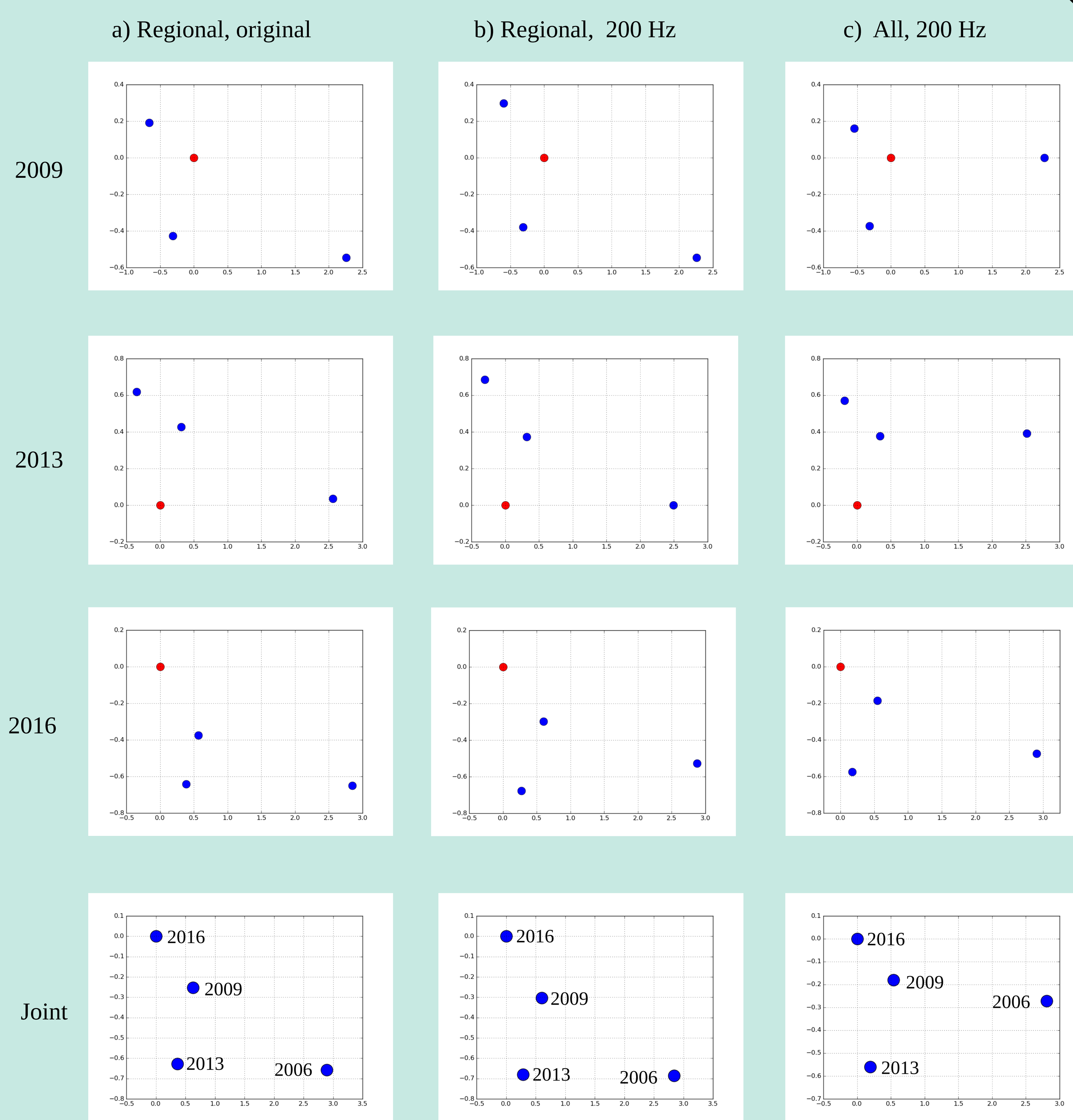

Fig. 10. Relative location calculated using 2009, 2013 and 2016 events as masters. The reference event is red. The joint relative location is shown in the bottom panels. a) Regional, original stations with original sampling rates. b) Regional stations resampled to 200 Hz. c) All available stations are resampled to 200 Hz. All locations are reduced to the epicentre of the 2016 DPRK (0,0).

Relative magnitude

$$dRM = \log(|S|/|M|) = \log|S| - \log|M|$$

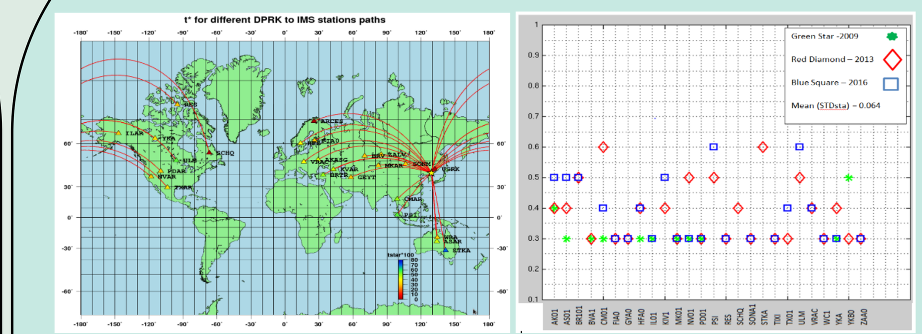

t* analysis was conducted based on results produced with synthetic modeling with hudson96 program. t* remains stable for the azimuths to the following stations:

NVAR, BR101, BVA1, GYA0, IL01, MK01, NV01, PD01, RES, SONA, TIXI, VRAC, WC1, ZAA0.

Low difference (δtstar = 0.1) corresponds to stations: AK01, KIV, PSI, TX01, ULM, YKA. Medium difference: (δtstar = 0.1-0.2) corresponds to stations AS01, CM01.
A color legend on a right map reflects t* values and the station triangles inherit this feature. Big difference in t* for stations with close azimuths and location (like ASAR and STKA) may evidence about a difference in crustal structure underneath receiver site and in a need of thorough local velocity model study.
A quantitative view of t* distribution is represented at a right figure.

Cepstral analysis*

Station	DPRK 2016 cepstral dt	DPRK 2016 cepstral Depth,km	DPRK 2013 cepstral dt, s	DPRK 2013 cepstral Depth,km	DPRK 2009 cepstral dt, s	DPRK 2009 cepstral Depth,km
AAK	0.17	0.46			0.15	0.41
AK01	0.35	0.96	0.17	0.46	0.20	0.54
ARA0	0.25	0.68	0.17	0.46	0.15	0.41
AS01	0.35	0.95	0.15	0.41	0.15	0.41
BR101	0.35	0.95	0.15	0.41	0.15	0.41
BVA1	0.25	0.68			0.13	0.35
CM01	0.15	0.41	0.15	0.41	0.15	0.41
FIA0	0.43	1.16	0.17	0.46	0.15	0.41
FITZ			0.17	0.46		
GYA0	0.18	0.49	0.15	0.41		
HFA0	0.18	0.49	0.16	0.43	0.16	0.43
IL01	0.20	0.54	0.15	0.41	0.13	0.35
KIV1	0.25	0.68	0.16	0.43		
KURK					0.20	0.54
KSRS	0.13	0.35	0.15	0.41	0.15	0.41
MJAR	0.15	0.41	0.15	0.41	0.15	0.41
MK01	0.25	0.68	0.12	0.32	0.13	0.35
NOA	0.17	0.46	0.18	0.49	0.15	0.41
NV01	0.32	0.86	0.16	0.43	0.17	0.46
PD01	0.34	0.92	0.15	0.41	0.10	0.27
RES	0.22	0.59	0.15	0.41		
SCHQ	0.38	1.03	0.17	0.46	0.15	0.41
SEY			0.17	0.46		
SONA0	0.18	0.49	0.17	0.46		
STKA	0.37	1.00	0.15	0.41	0.15	0.41
TIXI	0.27	0.73	0.15	0.41	0.13	0.35
TX01	0.39	1.05	0.15	0.41	0.12	0.32
ULM	0.17	0.46	0.15	0.41	0.17	0.46
USRK	0.18	0.49	0.17	0.46		
VRAC	0.27	0.73	0.15	0.41	0.15	0.41
WC1	0.32	0.86	0.18	0.49	0.17	0.46
YAK	0.17	0.46				
YKA	0.27	0.73	0.17	0.46		
ZAA0	0.17	0.46	0.15	0.41	0.14	0.38
Mean	0.25	0.68	0.16	0.43	0.15	0.41
St.Err.	0.09	0.23	0.01	0.03	0.02	0.06

*Preliminary estimates using geotool (NDC in a box IDC package) cepstral analysis option, Vp is the same for all cases.

M/S Sta	13/16 dRM	16/13 dRM	09/16 dRM	16/09 dRM	09/13 dRM	13/09 dRM	06/16 dRM	16/06 dRM	06/13 dRM	13/06 dRM	06/09 dRM	09/06 dRM
AKASG	-0.14	0.14	0.25	-0.25	0.44	-0.44	0.91	-0.90	1.05	-1.05	0.75	-0.75
ASAR	-0.23	0.23	0.28	-0.28	0.51	-0.50	0.84	-0.83	1.00	-1.01	0.51	-0.48
BRTR		0.17	0.27	-0.27	0.38	-0.38		-1.05		-1.13		-0.76
CMAR	-0.15	0.15	0.31	-0.30	0.46	-0.46						
ESDC	-0.30	0.30	0.08	-0.08	0.38	-0.38						
FINES	-0.06	0.05	0.29	-0.31	0.35	-0.36						
GERES	-0.09	0.09	0.34	-0.34	0.42	-0.42	1.04	-1.04	1.13	-1.12	0.75	-0.75
GEYT	-0.24	0.24										
ILAR	-0.04	-0.01	0.34	-0.34	0.39	-0.39						
KSRS	-0.09	0.09	0.30	-0.30	0.40	-0.40	0.95	-0.95	0.91	-0.97	0.52	-0.52
MKAR	-0.15	0.15	0.22	-0.22	0.37	-0.37	1.06	-0.92	1.21	-1.07	0.80	-0.80
NOA	-0.23	0.23										
NVAR	-0.09	0.09										
PDAR	-0.01	0.00										
PETK	-0.06				0.37	-0.34						
SONM	-0.18	0.18	0.29	-0.33	0.49	-0.52	0.87	-0.88	1.07	-1.06	0.58	-0.58
TXAR	0.00	-0.01	0.39	-0.39	0.41	-0.39						
USRK	-0.02	0.02	0.39	-0.39	0.41	-0.41						
WRA	-0.13	0.13	0.33	-0.33	0.43	-0.43	0.76	-0.76	0.84	-0.84	0.41	-0.41
ZALV	-0.15	0.15	0.26	-0.26	0.41	-0.41						
mean	-0.12	0.13	0.29	-0.29	0.41	-0.41	0.92	-0.92	1.03	-1.03	0.62	-0.63
stdev	0.09	0.09	0.08	0.08	0.04	0.05	0.11	0.10	0.13	0.09	0.15	0.15
mean REB	-0.13		0.28		0.40		0.97		1.09		0.56	
stdev REB	0.08		0.09		0.04		0.11		0.10		0.29	
REB mb diff	-0.10		0.31		0.41		0.74		0.84		0.43	

This table presents the relative magnitude estimates for all possible pairs of events in Master/Slave (M/S) configurations at all available stations. Larger event magnitude allows estimates at more stations with good SNR for waveform templates. Eight array stations measured all four events. Unfortunately, the closest station USRK did not work in 2006.

The relative magnitude is calculated as the logarithm of the ratio of L2-norms (lengths) of the slave and master. For the former, the length of time window is the same as in the master, which found that slave. The length of master template depends on the frequency band with the highest SNR at the averaged CC-trace.

Using an event as a master or slave may result in different RM absolute values because of a slight difference in the travel time residuals between channels for different locations of master events. This difference in small, however.

The dRM averaged over all available stations (mean) provides an accurate and reliable estimate of the relative size of two measured events. The standard error of the mean value (stdev) is also calculated in order to illustrate the level of residual magnitude scattering over stations. The average RM estimates are compared with those calculated by standard procedure from station magnitudes (mean REB and stdev REB) for the same event pairs. The difference of the network magnitudes (REB mb diff) for event pairs are also listed. N accurate and reliable

M/S Sta	13/16 CC	16/13 CC	09/16 CC	16/09 CC	09/13 CC	13/09 CC	06/16 CC	16/06 CC	06/13 CC	13/06 CC	06/09 CC	09/06 CC
AKASG	0.89	0.89	0.88	0.88	0.95	0.95	0.71	0.71	0.74	0.74	0.74	0.73
ASAR	0.94	0.94	0.9	0.9	0.95	0.96	0.75	0.75	0.71	0.72	0.68	0.67
BRTR		0.82	0.81	0.81	0.96	0.92		0.5		0.63		0.66
CMAR	0.97	0.96	0.87	0.86	0.89	0.89						
ESDC	0.59	0.58	0.56	0.56	0.6	0.59						
FINES	0.97	0.96	0.96	0.95	0.97	0.97						
GERES	0.98	0.97	0.97	0.97	0.97	0.97	0.56	0.55	0.57	0.56	0.57	0.58
GEYT	0.76	0.75										
ILAR	0.95	0.93	0.95	0.94	0.98	0.98						
KSRS	0.88	0.87	0.88	0.88	0.93	0.95	0.58	0.58	0.59	0.64	0.59	0.62
MJAR	0.8	0.8	0.79	0.8	0.9	0.91	0.58	0.58	0.63	0.63	0.72	0.73
MKAR	0.99	0.99	0.97	0.97	0.98	0.98	0.5	0.39	0.5	0.4	0.54	0.54
NOA	0.84	0.83										
NVAR	0.98	0.97										
PDAR	0.96	0.9										
PETK	0.47				0.53	0.51						
SONM	0.88	0.88	0.89	0.84	0.94	0.91	0.62	0.51	0.68	0.56	0.66	0.65
TXAR	0.92	0.92	0.9	0.9	0.88	0.91						
USRK	0.92	0.93	0.92	0.92	0.97	0.97						
WRA	0.91	0.91	0.88	0.88	0.97	0.97	0.88	0.88	0.89	0.9	0.9	0.91
ZALV	0.92	0.9	0.9	0.9	0.91	0.9						
mean	0.88	0.89	0.88	0.87	0.90	0.90	0.65	0.61	0.66	0.64	0.68	0.68
stdev	0.13	0.10	0.10	0.10	0.13	0.13	0.12	0.15	0.12	0.14	0.12	0.11

The applicability of relative location and dRM estimates depends on the similarity between master and slave signals. For higher cross correlation coefficients (CC), the master and slave are quite similar, and thus, close. That makes possible direct comparison of their RMS amplitudes (L2-norms). The presented CC estimates belong to the points with the highest SNR_{CC} and might be smaller than the peak absolute CC at the average CC-trace.

The estimates of CC for all pairs from four DPRK explosions at all available stations are listed in this table. For bigger events, CC is above 0.8-0.9 for almost all stations except PETK and GEYT. The mean CCs and their low standard errors illustrate the overall similarity between signals from DPRK 2009, 2013, and 2016.

The 2006 DPRK is smaller in size and relatively far from the bigger ones. Both conditions result in lower CC, as illustrated in the table. The mean CC is from 0.61 to 0.68 with the stdev estimates of 0.11 to 0.14 (8 to 9 stations involved). The highest CC was measured at large-aperture array WRA and station MKAR demonstrates just mediocre similarity between the 2006 and other explosions (CC from 0.39 to 0.54).

Preparatory Commission for the Comprehensive Nuclear-Test Ban Treaty Organization, Provisional Technical Secretariat, Vienna International Centre, P.O. Box 1200, A-1400 Vienna, Austria.
E-mail: ivan.kitov@ctbto.org